11. R. I. Kaiser, *Chem. Rev.* **102**, 1309 (2002).
12. C. A. Taatjes *et al.*, *Phys. Chem. Chem. Phys.* **7**, 806 (2005).
13. H. P. Reisenauer, G. Maier, A. Riemann, R. W. Hoffmann, *Angew. Chem. Int. Ed. Engl.* **23**, 641 (1984).
14. K. Komatsu, K. Kitagawa, *Chem. Rev.* **103**, 1371 (2003).
15. Z. Yoshida, *Pure Appl. Chem.* **54**, 1059 (1982).
16. R. Weiss, C. Priesner, H. Wolf, *Angew. Chem. Int. Ed. Engl.* **17**, 446 (1978).
17. R. Weiss, M. Hertel, H. Wolf, *Angew. Chem. Int. Ed. Engl.* **18**, 473 (1979).
18. M. Tamm, A. Grzegorzewski, F. E. Hahn, *J. Organomet. Chem.* **501**, 309 (1995).
19. H. Schumann *et al.*, *Angew. Chem. Int. Ed. Engl.* **36**, 2232 (1997).
20. Cyclopropenylidene transition metal complexes have been known since 1968 (*21*), and main group adducts were recently reported (*19*).
21. K. Öfele, *Angew. Chem. Int. Ed. Engl.* **7**, 950 (1968).
22. E. V. Patterson, J. F. Stanton, R. J. McMahon, *J. Am. Chem. Soc.* **119**, 5847 (1997).
23. G. Maier, T. Preiss, H. P. Reisenauer, B. A. Hess Jr., L. J. Schaad, *J. Am. Chem. Soc.* **116**, 2014 (1994).
24. The singlet-triplet energy gap and the ^{13}C NMR chemical shifts have been calculated at the RI-BP86/TZVP + ZPE correction level, and RI-BP86/TZVPP//RI-BP86/TZVP level, respectively, using Turbomole 5.7 (see www.ipc.uni-karlsruhe.de/tch/tch1/turbomole/index.en.html and references cited therein).
25. For discussions on carbene dimerization, see (*5*) and (*26*); cyclopropenylidene dimers, namely triafulvalenes, remain unknown (*27*).
26. M. Driess, H. Grutzmacher, *Angew. Chem. Int. Ed. Engl.* **35**, 828 (1996).
27. B. Halton, *Eur. J. Org. Chem.* **2005**, 3391 (2005).
28. A. J. Arduengo III, R. L. Harlow, M. Kline, *J. Am. Chem. Soc.* **113**, 361 (1991).
29. A. J. Arduengo III, J. Goerlich, W. Marshall, *J. Am. Chem. Soc.* **117**, 11027 (1995).
30. C. Heinemann, W. Thiel, *Chem. Phys. Lett.* **217**, 11 (1994).
31. R. W. Alder, P. R. Allen, M. Murray, A. G. Orpen, *Angew. Chem. Int. Ed. Engl.* **35**, 1121 (1996).
32. A. Igau, H. Grützmacher, A. Baceiredo, G. Bertrand, *J. Am. Chem. Soc.* **110**, 6463 (1988).
33. L. Nyulaszi, D. Szieberth, J. Reffy, T. Veszpremi, *Theochemistry* **453**, 91 (1998).
34. R. Weiss, C. Priesner, *Angew. Chem. Int. Ed. Engl.* **17**, 445 (1978).
35. Preparation methods and spectroscopic data for compounds **1c** and **4c** are available as supporting material on *Science* Online.
36. R. Breslow, *J. Am. Chem. Soc.* **79**, 5318 (1957).

37. We are grateful to NIH (grant R01 GM 68825) and RHODIA for financial support of this work. Metrical data for the solid-state structures of **1c** and **4c** are available free of charge from the Cambridge Crystallographic Data Centre under reference numbers CCDC-602795 and CCDC-602794, respectively.

Supporting Online Material

www.sciencemag.org/cgi/content/full/1126675/DC1
SOM Text
Tables S1 and S2
References

24 February 2006; accepted 31 March 2006
Published online 13 April 2006;
10.1126/science.1126675
Include this information when citing this paper.

The Sand Seas of Titan: Cassini RADAR Observations of Longitudinal Dunes

R. D. Lorenz,[1]* S. Wall,[2] J. Radebaugh,[1] G. Boubin,[1] E. Reffet,[1] M. Janssen,[2] E. Stofan,[3] R. Lopes,[2] R. Kirk,[4] C. Elachi,[2,5] J. Lunine,[1,2] K. Mitchell,[2] F. Paganelli,[2] L. Soderblom,[4] C. Wood,[6] L. Wye,[7] H. Zebker,[7] Y. Anderson,[2] S. Ostro,[2] M. Allison,[8] R. Boehmer,[2] P. Callahan,[2] P. Encrenaz,[9] G. G. Ori,[10] G. Francescetti,[11] Y. Gim,[2] G. Hamilton,[2] S. Hensley,[2] W. Johnson,[2] K. Kelleher,[2] D. Muhleman,[12] G. Picardi,[13] F. Posa,[14] L. Roth,[2] R. Seu,[13] S. Shaffer,[2] B. Stiles,[2] S. Vetrella,[11] E. Flamini,[15] R. West[2]

The most recent Cassini RADAR images of Titan show widespread regions (up to 1500 kilometers by 200 kilometers) of near-parallel radar-dark linear features that appear to be seas of longitudinal dunes similar to those seen in the Namib desert on Earth. The Ku-band (2.17-centimeter wavelength) images show ~100-meter ridges consistent with duneforms and reveal flow interactions with underlying hills. The distribution and orientation of the dunes support a model of fluctuating surface winds of ~0.5 meter per second resulting from the combination of an eastward flow with a variable tidal wind. The existence of dunes also requires geological processes that create sand-sized (100- to 300-micrometer) particulates and a lack of persistent equatorial surface liquids to act as sand traps.

The low gravity and dense atmosphere on Titan make it a favorable environment for aeolian transportation of material (*1*–*3*) in the sense that the windspeeds needed to saltate surface particles are rather low. However, until recently (*3*, *4*) it was thought that loose particles were difficult to generate and transport (erosive processes and wind, driven by the faint sunlight reaching Titan's surface, were expected to be weak) and would be susceptible to trapping by surface liquids.

Recently, numerical circulation models (*5*) incorporating the tide in Titan's atmosphere due to Saturn's gravity (*6*) (~400 times as strong as the moon's effect on Earth) show that near-surface winds may be dominated by this effect rather than solar heating, and periodically varying winds comparable with the transport threshold may result. The winds vary both in strength and direction. Data from Cassini (*7*, *8*) and from the Huygens probe (*9*) that landed on Titan in January 2005 show a very geologically varied surface, modified by a mix of processes including strong fluvial erosion, impact, and cryovolcanism. No evidence for large bodies of surface liquids has so far been found. Thus, the setting for aeolian transport now seems much more favorable.

Aeolian features appear on planetary surfaces at a wide range of scales, from cm-wide ripples to km-scale megadunes; imaging resolutions of better than 1 km are therefore required to observe them (*10*). Early large-scale near-infrared (near-IR) imaging at ~km resolution (*8*) by the Cassini Imaging Science Subsystem (ISS) indicated large-scale albedo patterns such as dark streaks and asymmetric edge contrasts (sharp westward boundaries and diffuse eastward ones) that were suggestive of net-eastward fluid transport of materials on Titan's surface, possibly by wind, but individual features could not be resolved. Radar imaging (*11*) on Cassini's T3 flyby (15 February 2005), however, with resolution down to 300 m, found many distinct radar-dark linear features (nicknamed "cat scratches") superposed on other geological units and having a spacing of 1 to 2 km and lengths of many tens of km, in a generally east-west orientation. These covered about 20% of that swath (which, like T8, covered ~1.8 million km^2, or almost 2% of Titan's surface), in patches with extents of up to 400 km.

Our most recent radar imaging (T8, 27 October 2005; see supporting online text) finds large expanses of these features, covering some 65% of that swath. Patches of these features vary from just a few km across to the width of the swath (~200 km), and one contiguous region is ~1500 km long. Furthermore, in some places in T8 the feature size, favorable geometry, and resolution of the observations allow the detection of bright topographic glints (Fig. 1). These

[1]Lunar and Planetary Laboratory, University of Arizona, Tucson, AZ 85721, USA. [2]Jet Propulsion Laboratory, California Institute of Technology, Pasadena, CA 91109, USA. [3]Proxemy Research, Bowie, MD 20715, USA. [4]U.S. Geological Survey, Flagstaff, AZ 86001, USA. [5]RADAR Team Leader, Jet Propulsion Laboratory, California Institute of Technology, Pasadena, CA 91109, USA. [6]Planetary Science Institute, Tucson, AZ 85719, USA and Wheeling Jesuit College, Wheeling, WV 26003, USA. [7]Stanford University, Stanford, CA 94305, USA. [8]Goddard Institute for Space Studies, National Aeronautics and Space Administration, New York, NY 10025, USA. [9]Observatoire de Paris, 92195 Meudon, France. [10]International Research School of Planetary Sciences, Universita' d'Annunzio, 65127 Pescara, Italy. [11]Facoltá di Ingegneria, 80125 Naples, Italy. [12]Division of Geological and Planetary Sciences, California Institute of Technology, Pasadena, CA 91125, USA. [13]Universitá La Sapienza, 00184 Rome, Italy. [14]Istituto Nazionale per la Fisica della Materia (INFM) and Dip. Interateneo di Fisica, Politecnico di Bari, 70126 Bari, Italy. [15]Agenzia Spaziale Italiana, 00131 Rome, Italy.

*To whom correspondence should be addressed. E-mail: rlorenz@lpl.arizona.edu

glints on the nearest side of the features, made visible by fortuitous geometry (the long axis of the dunes is roughly orthogonal to the radar look direction), suggest surfaces sloping toward the radar and show that the features are not merely thin streaks of material on the surface but have considerable positive topographic relief. Preliminary radarclinometric results [Titan's radar backscatter varies approximately as the cosecant (*7*) of the incidence angle; the incidence angle relative to a flat surface, typically 20° to 30°, is known from spacecraft navigation, and thus local variations of backscatter can be interpreted as a local tilt of the surface] yield slopes of 6° to 10° and heights of 100 to 150 m (Fig. 2).

Morphologically, the features resemble longitudinal dunes such as those found in the Namib and other terrestrial deserts (Fig. 2). Their height, longitudinal symmetry, superposition on other features, and the way they merge (forming "tuning fork" junctions) suggest that they are depositional. The interpretation as longitudinal dunes is supported by the way they divert and reconverge around topographic obstacles (Fig. 1). The asymmetric streamline pattern thus formed suggests that the net transport direction is generally eastward, with some regional variation (Fig. 3) and local deviations around elevated or bright topography (Figs. 1 and 4).

Dunes cover about 5% of the land surface on Earth, and longitudinal (linear, or sometimes "seif") dunes, where the material accumulates in lanes oriented along the mean transport direction, are among the most common type of dune (*12*, *13*), covering half to two-thirds of sand seas [in contrast, they are among the least-common dune type on Mars (*14*, *15*)]. Only in one place (Fig. 3) does a different duneform appear in our images so far. In flowing around an apparently large topographic rise, the dunes become transverse in form, before the longitudinal pattern resumes. Linear dunes are characteristic of a moderately variable windfield, typically one that varies around a mean or alternates between two widely spaced directions (*16*). Similarly, linear current ridges are formed on the terrestrial seabed by tidal currents (*17*). Purely unidirectional winds tend to form transverse dunes, whereas winds highly variable in direction form star dunes (*12*). On Titan, the wind regime that forms longitudinal dunes may be a natural result of the interaction of the fluctuating tidal windfield with the steady zonal (west-east) winds that prevail higher in the atmosphere (*18*). A substantial instantaneous meridional (north-south) component is implied, and the fact that dunes are not oriented exactly west-east everywhere also suggests a net meridional component over the long term. Whether or not the meridional component can be explained by other mechanisms, the presence of substantial meridional winds was not anticipated before the tidal model.

It is evident that topography has a substantial effect on near-surface winds—the dune orientation can veer by some 45° over just 10 km. Also, it may be that the bright region in Fig. 3 acts to straighten the windflow, suppressing the fluctuating component and yielding a unidirectional wind in which transverse dunes appear (see also figs. S1 and S2 for terrestrial analogs). The presence of the transverse features also, incidentally, rules out an erosional rather than depositional origin. Terrestrial dunes—the best examples being in the Namib and Sahara, with many other examples in the Australian and Arabian deserts—are typically a third as wide as their crest spacing (*13*), a geometry we also observe on Titan. This ratio indicates an ample sand supply—some terrestrial dune fields have much wider spacing.

The dunes' generally radar-dark appearance (also typical for radar images of terrestrial dunes; see supporting online text) is consistent with a smooth surface at our radar wavelength, suggesting that the dunes are made of fine

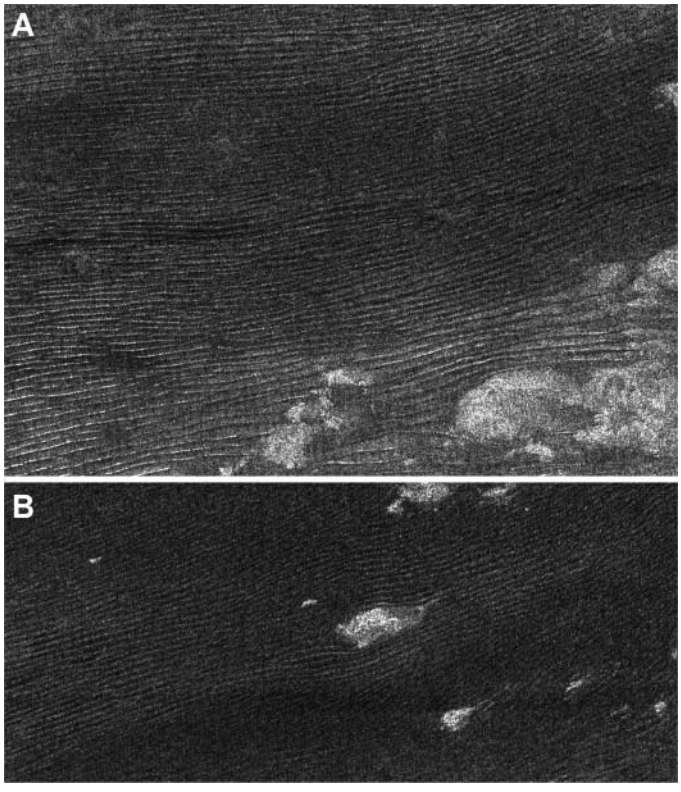

Fig. 1. (**A**) A 235 km by 175 km segment (north up) of the Belet sand sea at ~12°S, 100°W. Topographic glints are evidence of slopes facing the observer (radar illumination is from above). The subparallel orientation of the dunes and the 1:2 dune:interdune gap ratio are typical of longitudinal dunes on Earth. (**B**) Segment (235 km by 80 km) to the east of (A). Bright areas are small hills; the flow diverges around them and reconverges. A tail toward the right is evident in the lower hill, suggesting an east-northeast transport direction.

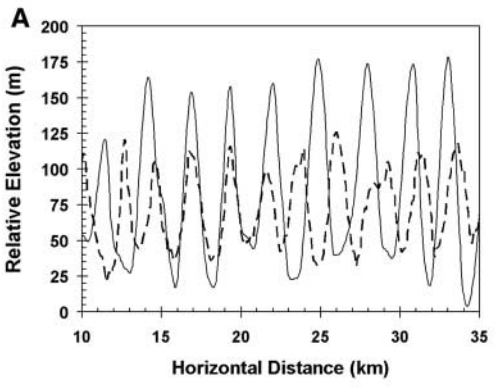

Fig. 2. (**A**) Radarclinometric profile of the Titan dunes shown in Fig. 1A (solid line). The spacing and height are typical of Namib desert dunes (B), a typical profile of which is shown by the dashed line (from Shuttle Radar Topography Mission data). (**B**) Handheld digital camera image of Namib sand sea showing undulating topography (see also fig. S2 and supporting online text.)

material with at most shallow ripples. Their composition is unknown—likely candidates are organic solids or water ice or some mixture thereof [silicates cannot be excluded but are less likely (*19*)]. At the large scale (50 km) observed by radar scatterometry, the sand seas are comparatively radar-dark too; in contrast, microwave radiometry indicates brightness temperatures 3 to 5 K above that of their surroundings, implying a high emissivity, i.e., low–dielectric constant material and little volume scattering, both consistent with a sand of ice/organic composition. It has been noted that the large low-albedo (optical and near-IR) regions on Titan appear to be concentrated around the equator (*8*, *20*). It also appears that radar sand seas and smaller dune fields correlate with low-latitude optically dark regions, notably Belet (Fig. 3) This in turn suggests that most or all of the equatorial dark regions may be covered in the dune material. One feature of the model tidal wind field is that the orbit-averaged winds at latitudes between 45°N and 45°S are directed equatorward [figure 6 of (*5*)]. An intriguing possibility is, therefore, that dark sediments may have been transported from higher latitudes to the equatorial sand seas by the tidal winds, forming this dark belt. Also, the predicted net meridional transport is weaker at 30° N (T3 region) where streaks are principally in an east-west direction, while there is a consistent east-northeast trend at 10°S (T8), where the average tidal wind has a northward flow of $\sim$0.25 ms^{-1}. Some high-latitude optically dark regions [e.g., the center of the TA swath (*7*)] have no apparent aeolian features—it may be that dark material blankets these areas, forming a sand sheet, but that it has not been swept into dunes either because winds are weaker or the ground is not dry. In this connection, our observation of dunes so far only at low latitudes is consistent with a recent model (*21*) of Titan's seasonally varying climate and methane hydrological cycle that predicts that Titan's equatorial regions should be dry, whereas higher latitudes have higher humidity and precipitation.

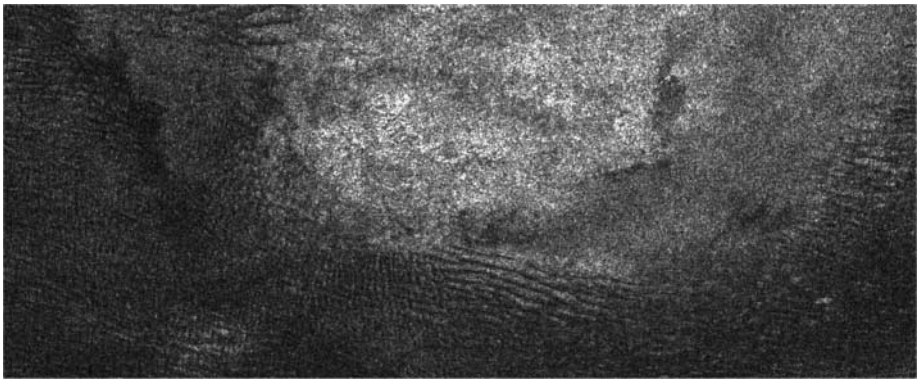

Fig. 3. A 515 km by 200 km segment of the T8 swath where the longitudinal dunes creeping from the left (west) encounter what appears to be a broad bright topographic rise. As the sand flows around this obstacle, it forms transverse dunes at the southwestern side before the longitudinal pattern resumes. Such a pattern confirms a depositional origin and is the only prominent example of dunes other than longitudinal ones observed so far.

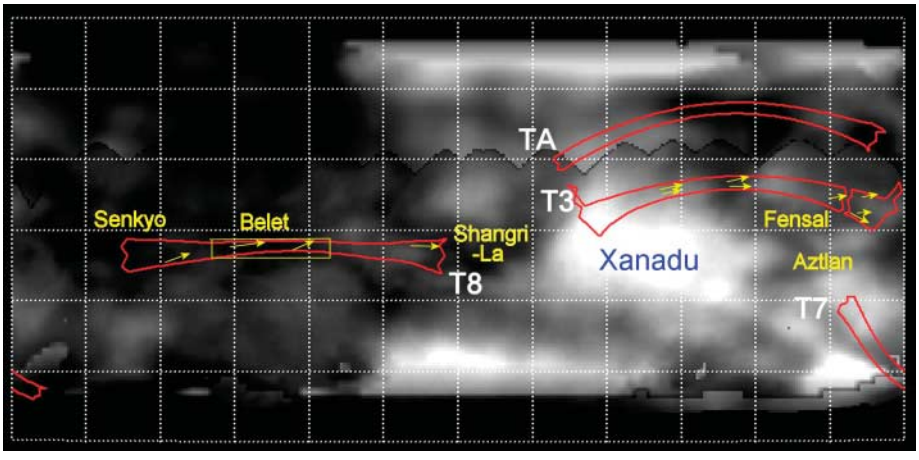

Fig. 4. Distribution and large-scale orientation of the aeolian features are indicated with yellow arrows, shown on a basemap (cylindrical projection, centered on the antisaturn point at 180°W, 30° grid spacing) derived from Hubble Space Telescope (HST) (*18*) and Cassini ISS (*8*) data. IAU names for dark albedo regions and the Xanadu bright terrain are indicated (a map with up-to-date names is maintained at http://planetarynames.wr.usgs.gov/index.html). Yellow box indicates the dunefield from which Fig. 1 is extracted. Red regions show radar imaging swaths to date (labeled TA, T3, T7, and T8); note the low-albedo regions along T7 and at the center of TA where no aeolian features were seen—all at latitudes around 45° where winds may be low. The directions indicated by the dunes appear to deviate around bright areas, suggesting that these may act as topographic obstacles to flow.

Sand transport for dune formation occurs by a wind-driven bouncing process called saltation. The optimum particle diameter (*1*–*3*) for saltation on Titan is $\sim$0.18 to 0.25 mm (larger particles have a higher weight:area ratio and are thus more difficult for wind to lift; smaller particles tend to clump together—there is thus an optimum size for which the threshold windspeed for transport by saltation is a minimum). The ease of transport in Titan's low gravity and thick atmosphere makes the optimum size somewhat larger than for Earth, Venus, and Mars (75, 75, and 115 μm, respectively), and the freestream windspeeds required for saltation are $\sim$0.1 to 0.7 ms^{-1} (*22*).

Near-surface winds predicted by the tidal model (*5*) are $\sim$0.5 ms^{-1}. Doppler tracking of the Huygens probe (*18*) indicates that winds in the lowest 5 km of descent were $\sim$1 ms^{-1}. Optical tracking by the Descent Imager and Spectral Radiometer experiment (*9*) permitted the Huygens probe's drift in the wind to be measured at $\sim$1 ms^{-1} near 2- to 3-km altitude, dropping to 0.3 ms^{-1} "close to the surface" (the last probe images from which such tracking is derived were acquired at altitudes of 200 to 300 m). Notably, in contrast to the eastward drift higher in the atmosphere, the wind near the surface blew the probe in a west-northwest direction. An analysis of the advective cooling of the Huygens probe (*23*) suggests that winds in the lowest 1 m were $\sim$0.2 ms^{-1} or less for the hour observed on the surface. It is likely that wind stress exceeds the transport threshold for only a small fraction of the time, but even the data at hand suggest winds broadly comparable with the saltation thresholds.

It is not clear how sand may be produced on Titan (*4*) because the thick atmosphere tends to inhibit explosive volcanism and many erosive processes. However, images from the Huygens probe (*9*) show clear evidence of fluvial activity at the landing site (9°S, 192°W), including rounded boulders, suggesting that particles can be generated in this way. Inspection of our radar images also indicates a number of areas where fluvial channels are present (*24*). Although channels and dunes can be within some tens of km of each other, we have so far not observed clear superposition of one on the other (*11*), nor have we so far identified obvious sand source regions anywhere. As on Earth, dunes may be formed on geologically short time scales (see supporting online text).

The existence of these dunes, their pristine appearance, and their superposition on other features tells us that in the geologically recent past, and quite probably the present, fine-grained and nonsticky (i.e., "dry") material has been moved across Titan's surface by wind. Because the net transport direction appears inclined at a small angle to eastward, it seems that if sand has migrated across large latitude ranges, the sand has circumnavigated Titan several times while doing so, apparently supporting a tidal wind model and arguing for an absence of standing liquids that would trap the sand [an absence of low-latitude lakes is also indicated by the lack of detection of specular reflections (*25*)]. The extent of the sand seas requires an origin for $\sim 10^4$ to 10^5 km^3 of sand-sized material, considerably more than would be produced by impact ejecta (*3*). It may be that fluvial erosion of ice bedrock by liquid methane is able to produce this fine material. This would then somehow have to dry out, placing constraints on Titan's meteorology. An alternative origin, perhaps supported by the optically dark appearance of the sand seas, is Titan's stratospheric methane photochemistry, which over 4.5 billion years of solar system history may have produced up to 10^6 to 10^7 km^3 of hydrocarbons and nitriles, 10% of which would be solid (*26*). At issue is how this organic material is sorted and modified to produce the equivalent (in size and material properties) of sand.

Much work remains to fully characterize the distribution, morphology, and composition of these features in data already acquired and the much larger data sets anticipated in Cassini's nominal and extended missions from RADAR and from other instruments, and to relate the features to the windfield and planetary-scale cycles of sediment generation and transport. However, the morphology of these beautiful features, familiar to us from terrestrial arid regions, is a comforting sign that even though the environment and working materials on Titan are exotic, the physical processes that shape Titan's surface (*19*) can be understood and studied here on Earth.

References and Notes

1. M. Allison, in *Proceedings Symposium on Titan, Toulouse, France, 9-12 September 1991*, B. Kaldeich, Ed. (European Space Agency SP-338, Noordwijk, Netherlands, 1992), pp. 113–118.
2. R. Greeley, J. Iverson, *Wind as a Geological Process* (Cambridge Univ. Press, Cambridge, 1985).
3. R. D. Lorenz, J. I. Lunine, J. A. Grier, M. A. Fisher, *J. Geophys. Res. (Planets)* **88**, 26377 (1995).
4. R. D. Lorenz, J. Mitton, *Lifting Titan's Veil* (Cambridge Univ. Press, Cambridge, 2002).
5. T. Tokano, F. M. Neubauer, *Icarus* **158**, 499 (2002).
6. R. D. Lorenz, in *Proceedings Symposium on Titan, Toulouse, France, 9-12 September 1991*, B. Kaldeich, Ed. (European Space Agency SP-338, Noordwijk, Netherlands, 1992), pp. 119–123.
7. C. Elachi *et al.*, *Science* **308**, 970 (2005).
8. C. C. Porco, *Nature* **434**, 159 (2005).
9. M. G. Tomasko *et al.*, *Nature* **438**, 765 (2005).
10. R. Greeley, *Planetary Landscapes* (Allen and Unwin, Boston, MA, 1987).
11. C. Elachi *et al.*, *Nature,* in press.
12. N. Lancaster, *The Geomorphology of Desert Dunes* (Routeledge, London, 1995).
13. R. Bagnold, *Physics of Wind-Blown Sand and Desert Dunes* (Methuen, London, 1941).
14. P. Lee, P. C. Thomas, *J. Geophys. Res.* **100**, 5381 (1995).
15. K. S. Edgett, M. C. Malin, *Lunar Planet. Sci.* **XXXI**, 1070 (2000).
16. D. Rubin, H. Ikeda, *Sedimentology* **37**, 673 (1990). See also (*27*).
17. J. M. Huthnance, *Estuarine Coastal Shelf Sci.* **14**, 79 (1982).
18. M. K. M. Bird, *Nature* **438**, 800 (2005).
19. R. D. Lorenz, J. I. Lunine, *Planet. Space Sci.* **53**, 557 (2005).
20. P. H. Smith *et al.*, *Icarus* **119**, 336 (1996). See also (*28*, *29*).
21. P. Rannou, F. Montmessin, F. Hourdin, S. Lebonnois, *Science* **311**, 201 (2006).
22. Transport occurs when the wind's friction speed U_* exceeds the threshold friction speed for saltation U_{*t}. U_* is a measure of wind stress that is related to the roughness-dependent drag coefficient C_d (typically 0.002 to 0.01) and the freestream windspeed U as $(U_*/U)^2 \sim C_d$; thus, the freestream threshold speed is ~10 to 25 times the friction speed. The optimum threshold speed has been estimated (*1–3*), depending on assumed density, etc., as $U_{*t} \sim 0.01$ to 0.03 ms^{-1}, and thus dune formation requires freestream windspeeds of 0.1 to 0.7 ms^{-1}. The corresponding Reynolds number range is 15 to 100.
23. R. D. Lorenz, *Icarus,* in press.
24. See http://photojournal.jpl.nasa.gov/catalog/PIA07366.
25. R. A. West, M. E. Brown, S. V. Salinas, A. H. Bouchez, H. G. Roe, *Nature* **436**, 670 (2005).
26. Y. L. Yung, M. A. Allen, J. Pinto, *Astrophys. J. Suppl.* **55**, 465 (1984).
27. S. Fryberger, G. Dean, in *A Study of Global Sand Seas*, E. D. McKee, Ed. (U.S. Geol. Surv. Prof. Pap. 1052, U.S. Government Printing Office, Washington, DC, 1979), pp. 137–169.
28. M. Hartung *et al.*, *Astron. Astrophys.* **421**, L17 (2004).
29. H. G. Roe *et al.*, *Geophys. Res. Lett.* **31**, L17S03 (2004).

30. We gratefully acknowledge those who designed, developed, and operate the Cassini/Huygens mission. The Cassini/Huygens Project is a joint endeavor of NASA, the European Space Agency (ESA), and the Italian Space Agency (ASI) and is managed by the Jet Propulsion Laboratory, California Institute of Technology, under a contract with NASA.

Supporting Online Material

www.sciencemag.org/cgi/content/full/312/5774/PAGE/DC1
Materials and Methods
SOM Text
Figs. S1 and S2

30 November 2005; accepted 22 February 2006
10.1126/science.1123257

Interstellar Chemistry Recorded in Organic Matter from Primitive Meteorites

Henner Busemann,[1]* Andrea F. Young,[1] Conel M. O'D. Alexander,[1] Peter Hoppe,[2] Sujoy Mukhopadhyay,[1]† Larry R. Nittler[1]

Organic matter in extraterrestrial materials has isotopic anomalies in hydrogen and nitrogen that suggest an origin in the presolar molecular cloud or perhaps in the protoplanetary disk. Interplanetary dust particles are generally regarded as the most primitive solar system matter available, in part because until recently they exhibited the most extreme isotope anomalies. However, we show that hydrogen and nitrogen isotopic compositions in carbonaceous chondrite organic matter reach and even exceed those found in interplanetary dust particles. Hence, both meteorites (originating from the asteroid belt) and interplanetary dust particles (possibly from comets) preserve primitive organics that were a component of the original building blocks of the solar system.

Carbonaceous chondrites, the most primitive meteorites, and interplanetary dust particles (IDPs), primitive dust collected in Earth's stratosphere, contain up to ~2 and ~35 weight percent C in organic matter, respectively. This organic matter may represent an important source of prebiotic molecules that were essential for the origin of life on Earth (*1*). Most of the organic matter is insoluble in demineralizing acids and organic solvents, and this proportion is probably macromolecular (*1*). Isotope anomalies in H and N suggest that this insoluble organic matter (IOM) is probably interstellar material that, like other presolar materials, has survived the formation of the solar system to be incorporated into planetesimals (*2–6*), but it may also include material that formed in the cold outer regions of the solar protoplanetary disk (*7*). Heating, mixing, and chemical reactions in the collapsing protosolar cloud, in the protoplanetary disk, and during accretion of the parent bodies of meteorites and IDPs could have altered—or erased—the initial isotope signatures of interstellar IOM. Aqueous alteration and thermal metamorphism on the parent bodies of meteorites and IDPs have further modified the organic carriers of these

[1]Department of Terrestrial Magnetism, Carnegie Institution of Washington, 5241 Broad Branch Road, NW, Washington, DC 20015, USA. [2]Max-Planck-Institut für Chemie (Otto-Hahn-Institut), Becherweg 27, D-55128 Mainz, Germany.

*To whom correspondence should be addressed. E-mail: busemann@dtm.ciw.edu

†Present address: Department of Earth and Planetary Sciences, Harvard University, 20 Oxford Street, Cambridge, MA 02138, USA.